The American Journal of Pathology, Vol. 183, No. 5, November 2013

The American Journal of
PATHOLOGY
ajp.amjpathol.org

STEM CELLS, TISSUE ENGINEERING, AND HEMATOPOIETIC ELEMENTS

Reactivation of NCAM1 Defines a Subpopulation of Human Adult Kidney Epithelial Cells with Clonogenic and Stem/Progenitor Properties

Ella Buzhor,[*†] Dorit Omer,[*†] Orit Harari-Steinberg,[*†] Zohar Dotan,[‡] Einav Vax,[*†] Sara Pri-Chen,[*§] Sally Metsuyanim,[*¶] Oren Pleniceanu,[*†] Ronald S. Goldstein,[¶] and Benjamin Dekel[*†‖]

From the Pediatric Stem Cell Research Institute and the Division of Pediatric Nephrology,[‖] Safra Children's Hospital, the Sheba Center for Regenerative Medicine,[†] the Department of Urology,[‡] and the Maurice and Gabriela Goldschleger Eye Research Institute,[§] Sheba Medical Center, Tel Hashomer, Sackler Faculty of Medicine, Tel Aviv University, Ramat-Gan; and the Mina and Everard Goodman Faculty of Life Sciences,[¶] Bar-Ilan University, Ramat-Gan, Israel*

Accepted for publication July 22, 2013.

Address correspondence to Benjamin Dekel, M.D., Ph.D., Pediatric Stem Cell Research Institute, Edmond and Lili Safra Children's Hospital, Sheba Medical Center, Tel Hashomer, 52621, Israel. E-mail: benjamin.dekel@gmail.com or binyamin.dekel@sheba.health.gov.il.

The nephron is composed of a monolayer of epithelial cells that make up its various compartments. In development, these cells begin as mesenchyme. NCAM1, abundant in the mesenchyme and early nephron lineage, ceases to express in mature kidney epithelia. We show that, once placed in culture and released from quiescence, adult human kidney epithelial cells (hKEpCs), uniformly positive for CD24/CD133, re-express NCAM1 in a specific cell subset that attains a stem/progenitor state. Immunosorted NCAM1$^+$ cells overexpressed early nephron progenitor markers (*PAX2*, *SALL1*, *SIX2*, *WT1*) and acquired a mesenchymal fate, indicated by high vimentim and reduced E-cadherin levels. Gene expression and microarray analysis disclosed both a proximal tubular origin of these cells and molecules regulating epithelial–mesenchymal transition. NCAM1$^+$ cells generated clonal progeny when cultured in the presence of fetal kidney conditioned medium, differentiated along mesenchymal lineages but retained the unique propensity to generate epithelial kidney spheres and produce epithelial renal tissue on single-cell grafting in chick CAM and mouse. Depletion of NCAM1$^+$ cells from hKEpCs abrogated stemness traits *in vitro*. Eliminating these cells during the regenerative response that follows glycerol-induced acute tubular necrosis worsened peak renal injury *in vivo*. Thus, higher clone-forming and developmental capacities characterize a distinct subset of adult kidney-derived cells. The ability to influence an endogenous regenerative response via NCAM1 targeting may lead to novel therapeutics for renal diseases. *(Am J Pathol 2013, 183: 1621–1633; http://dx.doi.org/10.1016/j.ajpath.2013.07.034)*

Kidney disease is a major worldwide health burden. Given the limited number of treatments currently available, discovering novel ways to stimulate kidney repair is an important therapeutic goal. Many adult tissues (such as skin, the hematopoietic system, and the intestine) are considered to harbor cells that self-renew and differentiate to form clones of stem, progenitor, and mature cells of the organ, fitting within the criteria of tissue-specific multipotential stem cells.[1–4] In contrast to these rapidly cycling organs, parenchymal cells of the kidney are considered to be mostly static under steady-state conditions and can be induced to divide only under very specific conditions, limiting the overall regenerative capacity of the nephron, the kidney's functional unit.[5] All nephron epithelia arise from a self-renewing nephron progenitor population that resides in the metanephric mesenchyme of the developing kidney's nephrogenic zone, specifically in the condensed mesenchyme that interacts with the ureteric bud, the precursor for the collecting system and undergoes mesenchymal–epithelial transition (MET). With

Supported by Israel Science Foundation grant no. 1139/07; the Israel Ministry of Industry 'NOFAR' program; Wolfson Clore Mayer; Tel Aviv University Stem Cell Research Center; and the Sackler School of Medicine, Tel Aviv University (all to B.D.).

E.B. and D.O. contributed equally to this work.

This study was performed in partial fulfillment of the requirements for the Ph.D. degree (E.B.).

http://dx.doi.org/10.1016/j.ajpath.2013.07.034

the completion of mammalian nephrogenesis (gestational week 34 in humans, 2 postnatal weeks in mice), this undifferentiated nephron-forming progenitor population is entirely exhausted. Therefore, in contrast to fish,[6] no progenitor population with nephrogenic potential similar to the metanephric mesenchyme or condensed mesenchyme physiologically exists in the mammalian adult kidney.[7,8]

Using microarrays, we have previously characterized the renal epithelial progenitor population of the developing human kidney.[9] Our results showed expression of a set of genes, including transcription factors that specify nephron lineage and are considered nephron progenitor markers,[10,11] a polycomb group, and Wnt pathway molecules concomitant with several surface antigens such as NCAM1. After validation by fluorescence-activated cell sorting (FACS) analysis, we demonstrated the usefulness of NCAM1 for immunoselection strategies and cell sorting of specific human developmental renal progenitor subsets.[9,12,13] After cessation of nephrogenesis, the early nephron progenitor markers are down-regulated in both murine kidneys[7] and human[8] kidneys. Similarly, NCAM1, which is strongly expressed in the condensed mesenchyme, nephrogenic zone, and in Wilms' tumor progenitor blastema, is not expressed in mature kidney epithelia after nephron differentiation.[12–15]

Here, we show that isolates of human kidney epithelia grown under adherent conditions proliferate and activate NCAM1 in a specific cell subset showing early renal stem/progenitor characteristics and function. The *in vitro* identification of distinct NCAM1$^+$ clone-forming cells and the possible beneficial role of NCAM1$^+$ cells in regenerating kidney epithelia *in vivo* suggest NCAM1 as a target for manipulation for an enhanced regenerative response.

Materials and Methods

hKEpC Cultures

Normal human adult kidney samples were retrieved from borders of renal cell carcinoma tumors from patients undergoing partial or total nephrectomy at Sheba Medical Center and Wolfson Hospital. This procedure was performed after approval by the local ethical committee and signed informed consent from the patient. The samples were minced in Hanks' balanced salt solution, soaked in collagenase for 2 hours, and then cultured in serum-containing medium (SCM), which consisted of Iscove's modified Dulbecco's medium supplemented with 10% fetal bovine serum, 1% L-glutamine, 1% penicillin–streptomycin, and the following growth factors: 50 ng/mL bFGF, 50 ng/mL EGF, and 5 ng/mL SCF (R&D Systems, Minneapolis, MN). Serum-free medium (SFM) consisted of 500 mL Dulbecco's modified Eagle's medium/F12 (DMEM/F12, 1:1; Life Technologies, Carlsbad, CA), 1% penicillin–streptomycin, 2 mL B27 supplement (Life Technologies), 4 μg/mL heparin, 1% nonessential amino acids (Life Technologies), 1% sodium pyruvate (Life Technologies), 1% L-glutamine, 1 mL lipid mix (Sigma-Aldrich, St. Louis, MO), 5 mL 100× N2 supplement (Life Technologies), 5 mL growth factor mix [200 mL of growth factor mix containing 100 mL DMEM/F12, 4 mL 30% glucose, 200 mg transferrin, 50 mg insulin in 20 mL of water, 19.3 mg putrescine in 20 mL distilled water, 200 μL sodium selenate (0.3 mmol/L stock), 20 μL progesterone (2 mmol/L stock)], 10 ng/mL FGF, and 20 ng/mL EGF. Sphere formation was tested by seeding the cells in polyHEMA (Sigma-Aldrich) precoated plates in SFM. Fetal kidney conditioned medium (FKCM) was obtained by combining SCM and supernatants from fetal kidney cultures (cultured in SCM) of passages 1 to 3 at a 1:1 ratio.

Cell Preparation and Sorting

Monolayer cells were detached from culture plates with 0.25% trypsin (Life Technologies). Viable cell number was determined using Trypan Blue staining (Life Technologies). In magnetic-activated cell sorting (MACS), CD56 (NCAM1) microbeads (Miltenyi Biotec, Auburn, CA) were used for single-marker cell separation. Positive and negative fractions were separated using Mini or Midi MACS columns (Miltenyi Biotec), according to the manufacturer's protocol. In FACS sorting, cells were sorted with anti-NCAM–phycoerythrin (PE) (eBioscience, San Diego, CA) using a FACSAria fluorescence-activated cell sorter and FACSDiva software version 4.0 (BD Biosciences, San Jose, CA), as described previously.[14]

Gene Expression Analysis of the Separated Cell Fractions

Quantitative real-time RT-PCR (RT-qPCR) reactions were performed as described previously.[12,16] In brief, total RNA from cells was isolated using an RNeasy micro kit (Qiagen, Hilden, Germany; Valencia, CA), according to the manufacturer's instructions. cDNA was synthesized using a high-capacity cDNA reverse-transcription kit (Life Technologies) on total RNA. qPCR was performed using an ABI 7900HT sequence detection system (Life Technologies) in the presence of TaqMan gene expression master mix (Life Technologies), and PCR amplification was performed using gene-specific TaqMan gene expression assay premade kits. Each analysis reaction was performed in duplicate or triplicate. *GAPDH* and *HPRT1* were used as endogenous control throughout all experiments. Analysis was performed using the ΔΔCT method, which determines fold change in gene expression relative to a comparator sample. PCR results were analyzed using SDS RQ Manager software version 1.2 (Life Technologies).

Clonogenicity of hKEpCs

Limiting dilution assay was performed on total human adult kidney or separated NCAM1$^+$ versus NCAM1$^-$ cell fractions. In brief, sorted cells were plated in 96-well plates

(Greiner Bio-One, Frickenhausen, Germany) in 150 μL of culture medium, at 1 or 5 cells per well. The number of colonized wells was recorded after 2 to 4 weeks. Confluent viable clones of total hKEpCs were isolated and propagated.

Proliferation Assay

NCAM1$^+$ and NCAM1$^-$ cell fractions were subjected to CellTiter 96 AQ nonradioactive cell proliferation (Promega, Madison, WI), based on the novel tetrazolium compound 3-(4,5-dimethylthiazol-2-yl)-5-(3-carboxymethoxyphenyl)-2-(4-sulfophenyl)-2*H*-tetrazolium (MTS), according to the manufacturer's protocol. Wavelength for optical density is 450 nm.

In Vitro Differentiation Assays

Osteogenic differentiation of NCAM1$^+$ cells was performed in NH OsteoDiff medium (Miltenyi Biotec), according to the manufacturer's protocol. NCAM1$^+$ cells were seeded at a concentration of 7.5×10^3 cells per well (1 mL medium per well) in 24-well plates and were incubated for 10 days. Osteoblast detection was performed by staining for alkaline phosphatase activity with an alkaline phosphatase kit (Sigma-Aldrich), according to the manufacturer's protocol.

Adipogenic differentiation of NCAM1$^+$ cells was performed in NH AdipoDiff medium (Miltenyi Biotec), according to the manufacturer's protocol. NCAM1$^+$ cells were seeded at a concentration of 12.5×10^3 cells per well (1 mL medium per well) in 24-well plates and were incubated for 21 days. Adipocyte detection was performed by staining with Oil Red O solution (Sigma-Aldrich).

DMEM was used as a control for differentiation assessment in both assays.

Microarray Analysis

Human adult renal NCAM1$^+$ and NCAM1$^-$ cell fractions obtained from one adult donor were evaluated using Affymetrix HU GENE1.0ORD oligonucleotide arrays (Affymetrix technical note: Data sheet: GeneChip HuGene 1.0 ST Array System for Human, Mouse and Rat. Santa Clara, CA). Total RNA from each sample was used to prepare biotinylated target DNA, according to the manufacturer's recommendations. Target cDNA generated from each sample was processed using an Affymetrix Gene Chip instrument system [Affymetrix technical note: User Manual: GeneChip Whole Transcript (WT) Sense Target Labeling Assay. Santa Clara, CA]. The quality and amount of starting RNA was confirmed using agarose gel or by use of an Agilent 2100 Bioanalyzer (Agilent Technologies, Santa Clara, CA).

When scanning was done, array images were assessed by eye to confirm scanner alignment and the absence of significant bubbles or scratches on the chip surface. The signals derived from the array were assessed using various quality assessment metrics. Details of quality control are provided in the Affymetrix data sheet cited above. Gene-level RMA sketch algorithm [Affymetrix Expression Console and Partek Genomics Suite version 6.2 (Partek, St. Louis, MO)] was used for generation of crude data. Significantly changed genes were filtered as changed by at least twofold ($P = 0.05$). Genes were filtered and analyzed using unsupervised and supervised hierarchical cluster analysis [Partek Genomics Suite and Spotfire DecisionSite for Functional Genomics version 9.1.2 (TIBCO Spotfire, Somerville, MA)] to get a first assessment of the data. Further processing included functional analysis and over-representation calculations based on Gene Ontology and using the publicly available Database for Annotation, Visualization and Integrated Discovery and associated tools (DAVID tools version 6.7; *http://david.abcc.ncifcrf.gov*). Over-representation calculations were performed using the DAVID Ease tool, according to the Affymetrix technical notes cited above. Ingenuity Pathway Analysis software (IPA version 7; Ingenuity Systems, Redwood City, CA) was used for network analysis. The microarray data were deposited with the Gene Expression Omnibus (*http://www.ncbi.nlm.nih.gov/geo*; accession no. GSE49100).

Nephron Segment-Specific Staining of NCAM1$^+$ and NCAM1$^-$ Cell Fractions in Culture

Tubular segments were identified using the segment-specific markers. Proximal tubules were identified with biotinylated *Lotus tetragonolobus* lectin (LTA) (1:200, Vector Laboratories) and aminopeptidase A (ENPEP) (1:75; Sigma-Aldrich); distal tubules and collecting ducts were identified with biotinylated *Dolichos biflorus* agglutinin (DBA) (1:200; Vector Laboratories); and epithelial cells were identified with cytokeratin (1:250; Dako). Before staining, cells were fixed in ice-cold 95% ethanol−5% acetic acid for 10 minutes, washed in PBS, and blocked with 0.1% bovine serum albumin in PBS for 1 hour. Detection was performed with streptavidin Alexa Fluor 488 (1:1000, Jackson ImmunoResearch Laboratories) and anti-rabbit Alexa Fluor 488 (1:1000; Life Technologies). Slides were counterstained with ProLong Gold antifade reagent with DAPI (Life Technologies). Photomicrographs were made on a Nikon TI-E inverted microscope.

Immunotoxin (huN901-DM1) Assay *in Vitro*

Lorvotuzumab mertansine (alias huN901-DM1 or IMGN901) is a humanized version of the anti-CD56 antibody N901, conjugated to the highly cytotoxic maytansine derivative DM1 via a hindered disulfide linker[17] (ImmunoGen, Waltham, MA).

Estimation of the Proliferation Rate of hKEpCs

hKEpCs were cultured at concentrations of 500, 1000, 2000, and 4000 cells per well in 96-well plates. After 1, 3, 5, and 7 days in culture, cell proliferation was evaluated using the

MTS cell proliferation assay (Promega). Cell plating concentration (cells per well) for the huN901-DM1 assays was based on a sufficient amount of cells at the beginning of the experiment so as not to reach confluence (and therefore massive cell death) by the end of the experiment.

Determination of the LD_{50} of huN901-DM1 on hKEpCs

To determine the LD_{50} of huN901-DM1 for hKEpCs, cells were seeded in 96-well plates at 10^4 cells per well for 24 hours in growth medium, which was then replaced with medium containing the conjugate in a range of concentrations between 1.6 nmol/L and 1.675 μmol/L, with medium alone serving as a control. After a 5-day incubation period, cell survival was assessed by the MTS proliferation assay and LD_{50} was determined.

huN901-DM1 Assay

hKEpCs were seeded at 2×10^4 cells per well in six-well plates in duplicate and were treated with anti-NCAM antibody (huN901), anti-NCAM antibody conjugated with immunotoxin (huN901-DM1; 0.1 μmol/L), or control. On day 5 of treatment, cells from all groups were subjected to limiting dilution, sphere formation, FACS, and MTS assays.

Grafting hKEpC $NCAM1^+$ Cells on the Chick Embryo CAM

Grafting of hKEpC $NCAM1^+$ cells on the chick embryo CAM was performed as described previously.[16,18] In brief, fertile chicken eggs were obtained from a commercial supplier and incubated at 37°C. On day 9 or 10 of incubation, a window was opened in the shell, and the CAM was exposed. hKEp $NCAM1^+$ cells separated by MACS were suspended in 50 μL medium and Matrigel (BD Biosciences) (1:1 by volume) and pipetted into a plastic ring placed on the chorioallantoic membrane (CAM). The egg was then sealed with adhesive tape and returned to the incubator. After 1 week, the graft was removed, paraffin-embedded, and serially sectioned at 6 μm for histological and immunocytochemical analyses, as described previously.[16,18]

Grafting hKEpC $NCAM1^+$ Cells in NOD/SCID Mice

$NCAM1^+$ cells separated by MACS were suspended in 200 μL Matrigel (BD Biosciences) and were injected subcutaneously into NOD/SCID mice (Harlan Laboratories, Israel). At 14 days after injection, the grafts were removed, paraffin-embedded, and serially sectioned at 6 μm for histological and immunocytochemical analyses.

Induction of Acute Kidney Injury and $NCAM1^+$ Cell Injection

Acute kidney injury (AKI) was induced in female NOD/SCID mice by intramuscular injection with 50% hypertonic glycerol (Sigma-Aldrich) solution in water (9 μL/g body weight) after water deprivation for 22 hours. Controlled intramuscular injection of glycerol into the inferior hind limbs was performed under anesthesia (isoflurane inhalation; Abbott Laboratories, North Chicago, IL). Mice received an intravenous injection into the tail vein at 2 hours after glycerol injection, as follows: group 1, saline ($n = 8$); group 2, $NCAM1^+$ cells ($n = 7$, 1.5×10^6 cells; $n = 3$, 0.43×10^6); and group 3, $NCAM1^-$ cells ($n = 7$, 1.5×10^6 cells; $n = 3$, 0.43×10^6). Human adult kidney cells were obtained from three different patients. Blood samples from mice were collected for blood urea nitrogen (BUN) and creatinine measurements at 3 and 14 days after glycerol injection; the animals were then sacrificed.

Animal experiments were performed in adherence to the National Institutes of Health Guide for the Care and Use of Laboratory Animals (8th edition, 2011), after approval by the Institutional Animal Care and Use Committee.

Immunotoxin (huN901-DM1) Assay *in Vivo*

BALB/c mice (Harlan Laboratories) received an intravenous injection into the tail vein 2 hours after glycerol injection, as follows: group 1, saline ($n = 10$); group 2, huN901-DM1 (18 μg/g; $n = 10$); and group 3, huN901(18 μg/g; $n = 10$). Blood samples from mice were collected for creatinine measurements at 3 days after glycerol injection; the animals were then sacrificed.

For NCAM1 staining, mouse kidneys were harvested at 3 days after glycerol injection, paraffin-embedded, and serially sectioned at 6 μm for immunofluorescence analysis with anti-NCAM1 antibody (Epitomics, Burlingame, CA). For FACS analysis, injured mouse kidneys were soaked in collagenase for 1 hour and the cells were stained with huN901 and human-IgG—fluorescein isothiocyanate (Abcam, Cambridge, MA).

Genetic Cell Labeling

To establish genetically marked hKEpCs, HEK293 cells were initially transformed. HEK293 cells were maintained in DMEM supplemented with 10% fetal calf serum, L-glutamine, penicillin, and streptomycin (Biological Industries, Beit-Ha'emek, Israel), at 37°C in a 5% CO_2—enriched atmosphere. Cells were transfected using calcium phosphate with three lentiviral vectors: 7.5 μg pHR-CMV-mCherry, 5 μg ΔR8.2, and 2.5 μg pMD2.G. After 6 hours, the supernatants were replaced with 5 mL of fresh medium. Supernatants of transfected cells were supplemented with HEPES (pH 7.0; 50 mmol/L final concentration) and filtered through a 0.45-μm pore-size filter; 2 mL was placed on the targeted cells for 2 hours with the addition of 8 μg/mL Polybrene (hexadimethrine bromide; Sigma-Aldrich), and then 3 mL of fresh medium was added. These viral-like particles were used to infect hKEpCs (2×10^5 cells in 60-mm-diameter dishes). Expression of the mCherry reporter gene was analyzed at 2 days after infection.

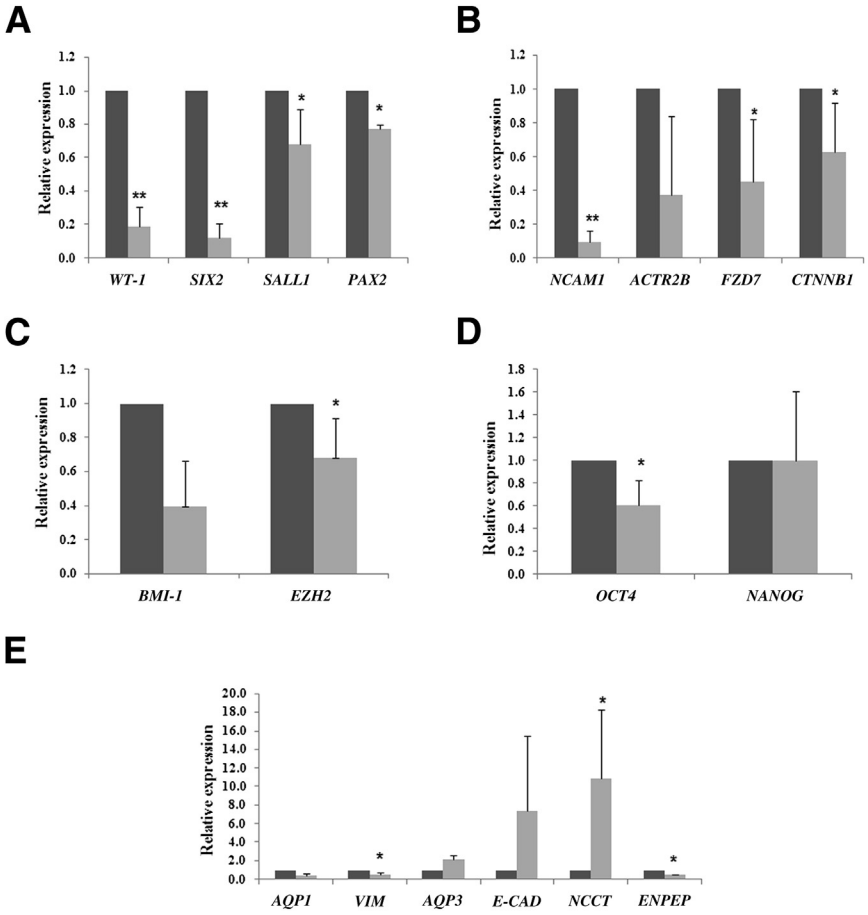

Figure 1 Gene expression analysis of NCAM1$^+$ (dark gray bars) versus NCAM1$^-$ (light gray bars) cell fractions. **A:** Nephron progenitor genes (*PAX2*, *SIX2*, *SALL1*, *WT1*). **B:** Genes of the Wnt pathway (*CTNNB1*, *FZD7*) and embryonic renal progenitor surface marker genes (*ACTR2B*, *FZD7*, *NCAM1*). **C:** Polycomb group genes (*BMI1*, *EZH2*). **D:** Pluripotency genes [*NANOG*, *POU5F1* (*OCT4*)]. **E:** Renal differentiation marker genes [vimentin (*VIM*), E-cadherin (*CDH1*), Na/Cl cotransporter (*NCCT*), aminopeptidase A (*ENPEP*), and aquaporins 1 and 3 (*AQP1*, *AQP3*)]. Differences in aquaporins 1 and 3 approached statistical significance ($P = 0.06$). Data are expressed as means ± SEM of at least three different experiments on human adult kidney from three different patients. *$P < 0.05$, **$P < 0.01$.

Human Cell Tracing in Mouse Kidney

mCherry-labeled hKEpCs were injected intravenously into NOD/SCID mice via the tail vein at 2 hours after glycerol-induced AKI. At 24 hours after cell injection, the animals were sacrificed. Both kidneys were surgically removed and were immediately analyzed with a CRi Maestro II *in vivo* imaging system (Caliper Life Sciences, Hopkinton, MA). Fluorescence images were obtained with an excitation wavelength of 465 nm and emission wavelength range of 500 to 800 nm.

RT-PCR of the Mouse Kidneys

RNA was isolated from the dissected kidneys using TRIzol reagent (Life Technologies) and then was reverse-transcribed as described above. Quantitative PCR was performed using a qPCR system for hGAPDH and mβ-actin, using gene-specific TaqMan gene expression assay premade kits (Life Technologies). The PCR products were analyzed by electrophoresis in 2.5% agarose gel and visualized by ethidium bromide staining.

Statistical Analysis

Statistical differences between two groups of data were compared by Student's *t*-test. For all statistical analyses, the level of significance was set as $P < 0.05$. Except as otherwise indicated, data are expressed as means ± SEM.

Results

NCAM1 Is Activated in Proliferative hKEpC

After the retrieval of a small specimen of human adult kidney tissue from nephrectomized patients, tissue was dissociated into a single-cell suspension and cultured at low densities (approximately 1 cell/cm^2) under adherent conditions in T75 flasks, to enhance clonal growth of hKEpCs.[16] Proliferative hKEpCs comprise several types of kidney epithelia. To determine whether proliferative hKEpCs express NCAM1 after reaching confluence, despite a lack of *in situ* expression in renal epithelia, we performed FACS analysis and found 15.9 ± 9.1% NCAM1 staining. Previous analysis has shown that putative renal stem-cell surface antigens CD24 and CD133,[19,20] as well as the epithelial differentiation marker EpCAM, are widely expressed in proliferative hKEpC[12] and therefore represent the entire growing culture, rather than a cell subset such as NCAM1.

NCAM1$^+$ Cells Overexpress Renal Progenitor Markers

Having determined that proliferative hKEpCs can be stimulated to express NCAM1, we characterized sorted NCAM1$^+$

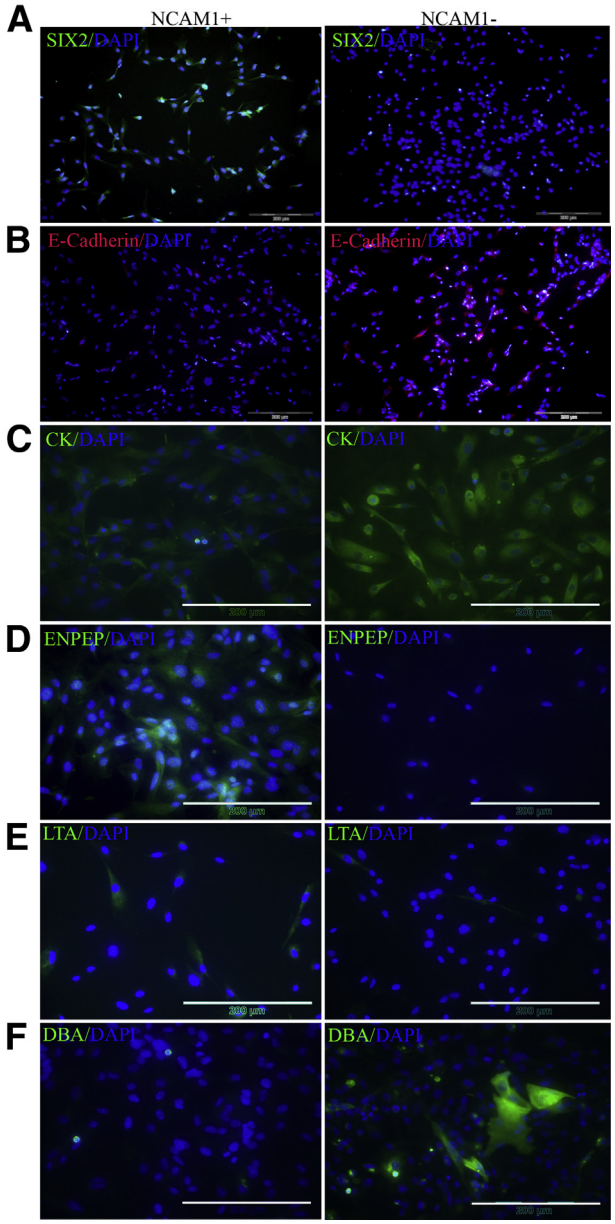

Figure 2 Expression of nephron segment-specific markers in NCAM1$^+$ and NCAM1$^-$ cell culture in representative micrographs of immunofluorescent staining of cell cultures at 1 day after separation. **A:** SIX2. **B:** E-cadherin. **C:** Cytokeratin (CK). **D:** Aminopeptidase A (ENPEP). **E:** LTA. **F:** DBA. Positively stained cells are green or red; nuclei are stained with DAPI (blue). Scale bar = 200 μm. Original magnification, ×20.

cells (Supplemental Figure S1) by qPCR for the expression of the following markers associated with renal stemness[10,21]: early nephron progenitors (*SIX2*, *SALL1*, *PAX2*, and *WT1*) (Figure 1A), early surface antigens (*FZD7*, *ACVR2B*) (Figure 1B),[11] polycomb group (*BMI1*, *EZH2*) (Figure 1C), Wnt pathway (β-catenin, *FZD7*) (Figure 1B), and the pluripotency and reprogramming factor *POU5F1* (alias *OCT4*) (Figure 1D). Analysis of proliferative hKEpCs generated from adult kidney from five different patients indicated significant overexpression of these genes in NCAM1$^+$ cells, compared with the negative fraction. Concomitantly, we observed high vimentin (*VIM*) and low E-cadherin (*CDH1*) levels in NCAM1$^+$ cells (Figure 1E), indicative of a more mesenchymal fate simulating earlier stages of renal development.

To test whether NCAM1$^+$ cells retain differentiation markers, we analyzed expression of markers that indicate various mature nephron compartments (Figure 1E). qPCR revealed elevated aminopeptidase A (*ENPEP*) and aquaporin 1 (*AQP1*) levels and low sodium/chloride cotransporter (*SLC12A3*; alias *NCCT*) and aquaporin 3 (*AQP3*) expression, indicating that NCAM1$^+$ cells most likely originate from the proximal tubule. Further interrogation of NCAM1$^+$ cells by immunofluorescence indicated enhanced SIX2 expression, as well as reduced levels of E-cadherin and pan-cytokeratin, compared with NCAM1$^-$ cells. Immunostaining of ENPEP and to a lesser extent LTA (proximal tubule markers), but not DBA (a marker of distal and collecting tubules), was more prominent in NCAM1$^+$ cells (Figure 2). Thus, a distinct lineage in proliferative hKEpCs may be activated to acquire progenitor markers.

Global Transcriptional Changes in NCAM1$^+$ Cells Show Reduced Expression of Genes Characteristic of Kidney Differentiation

Having identified specific characteristics of NCAM1$^+$ cells, we aimed to assess at a global level the transcriptional changes taking place after separation, based on NCAM1 expression. For this purpose, we separated NCAM1$^+$ and NCAM1$^-$ populations and compared their global gene expression profile using oligonucleotide microarrays. Unsupervised clustering (Partek Genomic Suite version 6.5) of the entire human microarray data set clearly distinguished between the two groups, indicating a different biological entity and fundamental difference in gene expression patterns (Figure 3). We identified 316 genes differentially expressed

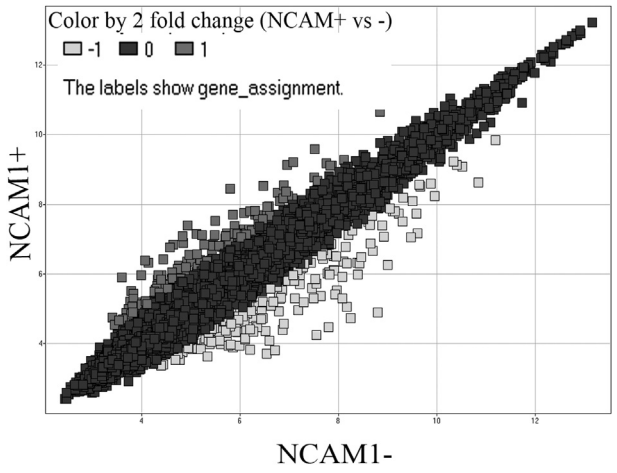

Figure 3 Microarray analysis of NCAM1$^+$ versus NCAM1$^-$ fractions of hKEpCs. Scatter plot of differentially expressed genes, those that were either up-regulated (142 genes) or down-regulated (174 genes) in the NCAM1$^+$ cell fraction at least twofold, compared with the NCAM$^-$ cell fraction.

Table 1 Gene Ontology Annotations for Up- and Down-Regulated Genes in the NCAM1$^+$ versus NCAM1$^-$ Subpopulations

GO Term	Count	%	*P* value
Biological processes			
Up-regulated			
Inflammatory response	13	11.40	1.54×10^{-6}
Acute inflammatory response	8	7.02	3.86×10^{-6}
Response to wounding	15	13.16	9.86×10^{-6}
Immune response	17	14.91	1.10×10^{-5}
Positive regulation of immune system process	10	8.77	2.84×10^{-5}
Response to oxygen levels	8	7.02	4.18×10^{-5}
Vasculature development	10	8.77	4.31×10^{-5}
Defense response	15	13.16	5.13×10^{-5}
Angiogenesis	8	7.02	5.70×10^{-5}
Regulation of cell activation	8	7.02	1.63×10^{-4}
Complement activation	5	4.39	1.69×10^{-4}
Positive regulation of response to stimulus	9	7.89	1.73×10^{-4}
Activation of plasma proteins involved in acute inflammatory response	5	4.39	1.85×10^{-4}
Blood vessel development	9	7.89	2.23×10^{-4}
Response to hypoxia	7	6.14	2.66×10^{-4}
Innate immune response	7	6.14	3.12×10^{-4}
Activation of immune response	6	5.26	4.01×10^{-4}
Positive regulation of immune response	7	6.14	4.06×10^{-4}
Regulation of lymphocyte activation	7	6.14	4.53×10^{-4}
Blood vessel morphogenesis	8	7.02	5.08×10^{-4}
Cell adhesion	14	12.28	7.04×10^{-4}
Biological adhesion	14	12.28	7.13×10^{-4}
Regulation of leukocyte activation	7	6.14	8.30×10^{-4}
Positive regulation of cell activation	6	5.26	8.58×10^{-4}
Complement activation, classical pathway	4	3.51	9.18×10^{-4}
Regulation of T cell activation	6	5.26	0.00109
Down-regulated			
Cell adhesion	21	13.82	6.92×10^{-6}
Biological adhesion	21	13.82	7.07×10^{-6}
Ectoderm development	10	6.58	1.01×10^{-4}
Defense response	17	11.18	1.87×10^{-4}
Epidermis development	9	5.92	3.22×10^{-4}
Immune response	17	11.18	6.67×10^{-4}
Taxis	8	5.26	7.39×10^{-4}
Chemotaxis	8	5.26	7.39×10^{-4}
Inflammatory response	11	7.24	9.16×10^{-4}
Lymphocyte chemotaxis	3	1.97	0.00175
Leukocyte migration	5	3.29	0.00194
Cell-substrate adhesion	6	3.95	0.0022
Positive regulation of cell adhesion	5	3.29	0.00234
Molecular function			
Up-regulated			
Water transporter activity	4	3.51	8.19×10^{-5}
Calcium ion binding	17	14.91	4.02×10^{-4}
Water channel activity	3	2.63	0.00287
Integrin binding	4	3.51	0.00744
RNA polymerase II transcription factor activity, enhancer binding	3	2.63	0.02862
GPI anchor binding	2	1.75	0.03344
Protein complex binding	5	4.39	0.04409
Solute:solute antiporter activity	3	2.63	0.05179
Symporter activity	4	3.51	0.06605
Wide pore channel activity	2	1.75	0.07211
Endopeptidase inhibitor activity	4	3.51	0.0755
Antiporter activity	3	2.63	0.07764
Peptidase activity, acting on L-amino peptides	8	7.02	0.07859
Peptidase inhibitor activity	4	3.51	0.08552
Polysaccharide binding	4	3.51	0.08681
Pattern binding	4	3.51	0.08681
Amine transmembrane transporter activity	3	2.63	0.08973
Peptidase activity	8	7.02	0.09416
Glucose transmembrane transporter activity	2	1.75	0.09704
Down-regulated: None			
Cellular components			
Up-regulated			
Extracellular region part	26	22.81	9.65×10^{-9}
Extracellular region	33	28.95	5.29×10^{-6}
Extracellular matrix	13	11.40	6.44×10^{-6}
Proteinaceous extracellular matrix	12	10.53	1.80×10^{-5}
Extracellular space	17	14.91	2.70×10^{-5}
Platelet alpha granule lumen	4	3.51	0.00316
Cytoplasmic membrane-bounded vesicle lumen	4	3.51	0.00386
Vesicle lumen	4	3.51	0.00438
Platelet alpha granule	4	3.51	0.0076
Extracellular matrix part	5	4.39	0.01004
Down-regulated			
Extracellular region	46	30.26	1.01×10^{-9}
Plasma membrane part	44	28.95	1.83×10^{-7}
Extracellular region part	27	17.76	2.84×10^{-7}
Extracellular space	21	13.82	2.75×10^{-6}
Plasma membrane	57	37.50	1.12×10^{-5}
Tight junction	6	3.95	4.99×10^{-4}
Occluding junction	6	3.95	4.99×10^{-4}
Integral to plasma membrane	23	15.13	8.13×10^{-4}
Intrinsic to plasma membrane	23	15.13	0.00109
High-density lipoprotein particle	4	2.63	0.00141

A detailed description of the microarray experiment is available through Gene Expression Omnibus at the National Center for Biotechnology Information at http://www.ncbi.nlm.nih.gov/geo, accession number: GSE49100. No down-regulated genes identified for molecular function.

by NCAM1$^+$ and NCAM1$^-$ cell fractions (>2.0-fold change, $P < 0.05$, analysis of variance), including 142 genes up-regulated and 174 down-regulated in NCAM1$^+$ cells, compared with NCAM1$^-$ cells (Figure 3). The 20 most

up-regulated genes and the 20 most down-regulated genes are listed in Supplemental Table S1.

To infer the function of the 316 differentially expressed genes, we used the Gene Ontology (GO) enrichment analysis tool and DAVID. The results provided compelling evidence for epithelial dedifferentiation and EMT, including down-regulation of E-cadherin, various keratins (*KRT7*, *KRT81*, and *KRT34*), and tight junction genes (*CLDN16*, *CLDN7*, *OCLN*, *CGN*, *MARVELD2*, *CLDN3*), all indicating epithelial development. Consistently, we detected strong down-regulation of *RBM35A* (now reclassified as *ESRP1*, epithelial splicing regulatory protein 1). Recently, the activation of the FGFR2/RBM35A signaling pathway has been shown to maintain epithelial integrity and be critical for regulating the EMT phenotype.[22,23] In addition, cell adhesion molecules were mostly down-regulated in NCAM1$^+$ cells, whereas *WNT5B*, which provides permissive cues for cell movement during development, was up-regulated,[24–27] suggesting enhanced migratory capacity of dedifferentiated cells.

The NCAM1$^+$ fraction showed up-regulation of a variety of functional proteins (eg, ion channels, water transporter activity) (Table 1). Close examination of this group revealed genes that specify proximal tubular function [bicarbonate (*SLC4A4*), phosphate (*SLC34A2*), glucose (*SLC2A9*, *SLC2A3*), urea (*SLC14A1*), and cationic amino acid (*SLC7A7*) transporters/cotransporters, as well as aminopeptidase A (*ENPEP*), aquaporin 1 (*AQP1*), and carbonic anhydrase IX (*CA9*)], reaffirming a proximal origin of NCAM1$^+$ cells. Finally, we observed up-regulation of gene groups that function in immune modulation and angiogenesis, which may be beneficial in the context of cell therapy (Table 1). Moreover, most transcriptional changes in our data set were noted in genes that regulate the extracellular compartment and may influence tissue remodeling (Table 1) (DAVID) ($P < 0.00001$).

NCAM1$^+$ Cells Exhibit Robust Clonogenicity, Mesenchymal Differentiation, Sphere-Formation Capacity, and Retain Ability to Produce Renal Epithelial Tissue

We next tested whether NCAM-expressing cells can be distinguished by *in vitro* stem/progenitor assays. Calibration experiments showed that hKEpCs cultured with human FKCM harbor enhanced clonogenic capacity (Supplemental Figure S2). We therefore assessed clonogenic potential by cloning single isolated NCAM1$^+$ and NCAM1$^-$ cells under these conditions in 96-well plates. Experiments were

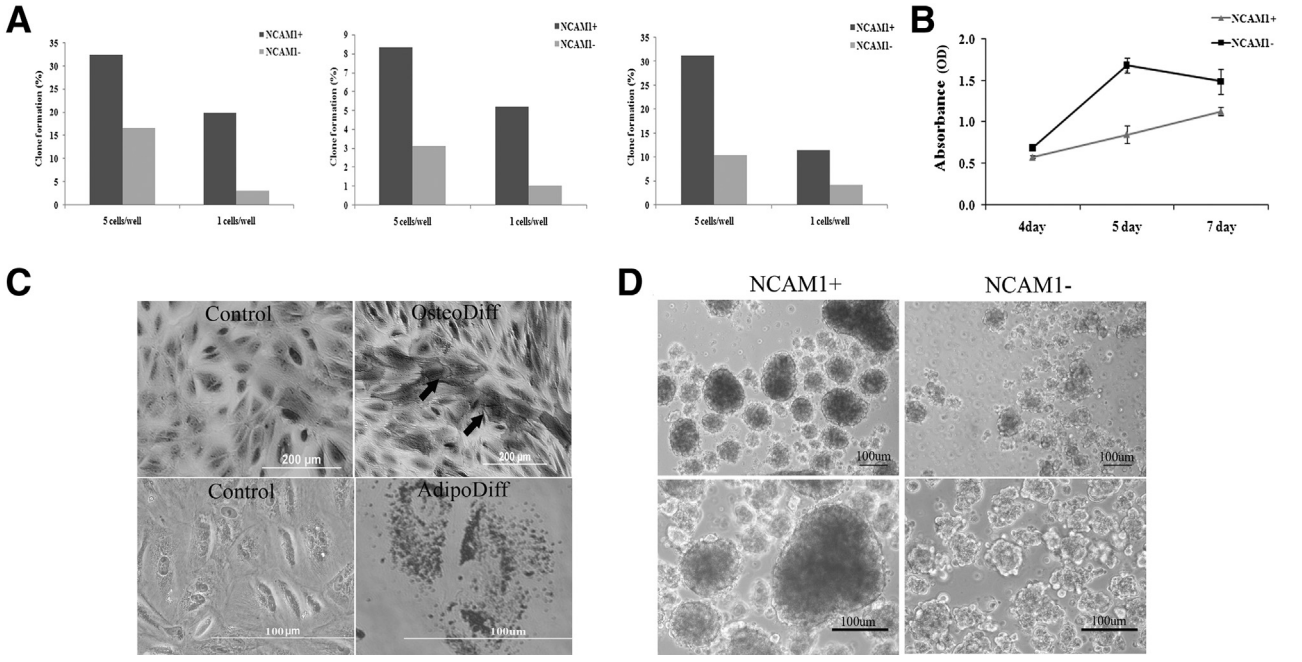

Figure 4 Functional analysis of NCAM1$^+$ and NCAM1$^-$ cells *in vitro*. **A:** Sorted human NCAM1$^+$ and NCAM1$^-$ cells were subjected to clone-formation assay performed in FKCM. Both NCAM1$^+$ and NCAM1$^-$ cells were plated at 1 and 5 cells per well. NCAM1$^+$ cells exhibited significantly higher clonogenic potential in all concentrations in all three experiments; cells originated from human adult kidney from three different patients. **B:** Sorted human NCAM1$^+$ and NCAM1$^-$ cells were subjected to MTS proliferation assay. Both NCAM1$^+$ and NCAM1$^-$ cell fractions were analyzed at 4, 5, and 7 days after sorting. NCAM1$^+$ cells exhibited decreased proliferation rates. Data are representative of three experiments performed in triplicate. **C:** Differentiation of NCAM1$^+$ cells into osteoblasts and adipocytes (**arrows** indicate positive staining). **Top row**: Representative micrographs of histochemical staining after 10 days in control medium (DMEM) and OsteoDiff medium. **Bottom row**: Representative micrographs of histochemical staining after 21 days in control medium (DMEM) and AdipoDiff medium. **D:** Sphere-formation assay. NCAM1$^+$ and NCAM1$^-$ cells isolated from low-passage cultures expanded *in vitro* exhibit exclusive capacity of the NCAM1$^+$ fraction to form well-defined spheres after 7 days under low-attachment culture conditions. Data are expressed as means ± SEM. Scale bars: 200 μm (**C**, **top row**); 100 μm (**C**, **bottom row**, and **D**). Original magnification: ×10 (**C**, **top row**); ×20 (**C**, **bottom row**, and **D**). *$P < 0.05$. OD, optical density.

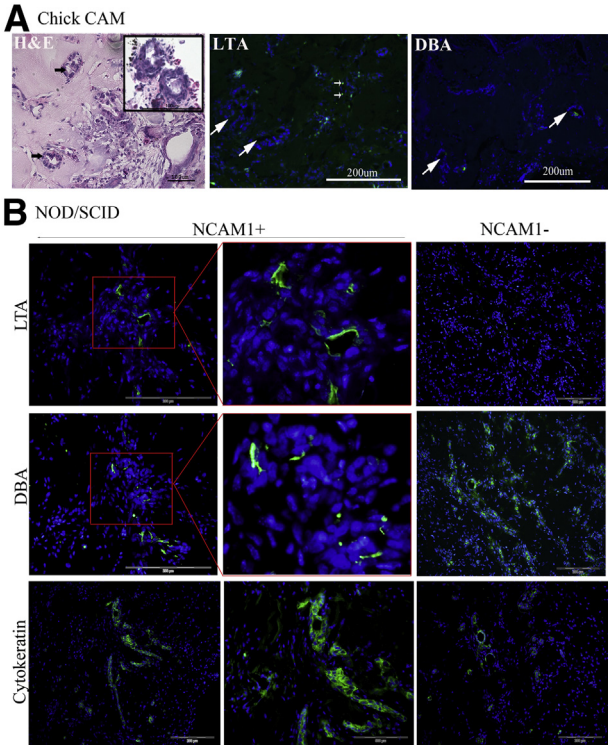

Figure 5 In vivo analysis of sorted human NCAM1$^+$ cells. Sorted NCAM1$^+$ cells (0.43×10^6) were grafted onto the chick CAM and assessed after 7 days. **A:** H&E staining of the grafts reveals tubular formation. LTA staining is positive (green) in unorganized cells (**small arrows**); no positive staining was detected in organized tubules (**large arrows**). No DBA staining was detected in tubules (**arrows**) or other structures. Nuclei were stained with DAPI (blue). **Boxed** regions are shown at higher magnification in the corresponding **middle** panels. **B:** NCAM1$^+$ and NCAM1$^-$ cells were injected subcutaneously into NOD/SCID mice and grafts were analyzed at 2 weeks after transplantation. Analysis of renal structures for expression of segment-specific antibodies reveals positive staining for LTA staining only in grafts derived from NCAM1$^+$ cells, but positive staining of DBA and cytokeratin in both NCAM1$^+$ and NCAM1$^-$ grafts. Scale bars: 100 μm (**A**, **right**); 200 μm (**A**, **middle** and **left**; **B**, **left** and **right**).

performed using cells from three different patients. Of the single NCAM1$^+$ cells, 3% to 16% divided and eventually filled the culture well with a confluent monolayer, whereas the majority of single NCAM1$^-$ cells did not (Figure 4A). Interestingly, a parallel analysis of proliferation rate using the MTS assay indicated reduced proliferation in NCAM1$^+$ cells (Figure 4B), indicating the highly clonogenic, slow-cycling nature of the cells. Proliferative hKEpCs grown under low-attachment conditions have been shown to produce kidney-spheres that elevate E-cadherin and recapitulate functioning kidney epithelial organoids.[16] It was therefore interesting to determine whether NCAM1$^+$ cells, which harbor propensity to a mesenchymal fate (high vimentin, low E-cadherin) (Figure 1E), as well as forced adipogenic and osteogenic differentiation with inductive culture medium (Figure 4C), exhibit this *in vitro* capacity. Immediately after sorting of low-passage cultures (P2), only NCAM1$^+$ cells generated kidney-spheres/organoids, whereas the NCAM1$^-$ fraction was devoid of this capacity (Figure 4D), suggesting that NCAM1$^+$ cells, although deviating toward mesenchyme, maintain *in vitro* plasticity and epithelial fate.

We further analyzed whether dedifferentiated NCAM1$^+$ could also redifferentiate to generate epithelial structures *in vivo* and grafted cells in the chick CAM assay and on transplantation into the subcutaneous space of NOD/SCID mice. Importantly, multipotential mesenchymal cells were completely devoid of tubulogenic potential on CAM grafting.[16] After 1 week, implantation of 0.43×10^6 NCAM1$^+$ cells into the CAM revealed large, well-defined grafts (Supplemental Figure S3A). H&E staining of graft sections revealed extensive morphogenesis into tubular structures (Figure 5A). These tubular structures did not express segment-specific kidney maturation markers (cytokeratin/MNF116, LTA, DBA). These markers appear only at late stages of human kidney development in differentiated structures (Supplemental Figure S3, C and D). Therefore, after dedifferentiation, the observed robust redifferentiation capacity of NCAM1$^+$ cells on the chick CAM may follow developmental MET, leading initially to generation of primitive tubular structures (devoid of maturation markers) reminiscent of early kidney development. In contrast to NCAM1$^+$ cells, less dedifferentiated NCAM1$^-$ cells were found to generate DBA$^+$ tubule structures after 1 week (Supplemental Figure S3B). Because the CAM model has a 1-week time limit for analysis, we used grafts developed in the NOD/SCID mouse for a 2-week period. At 2 weeks, NCAM1$^+$ cells reconstituted differentiated human cytokeratin$^+$ tubules (Figure 5B) and could generate both LTA$^+$ and DBA$^+$ type proximal and distal tubules, in contrast with NCAM1$^-$ cells, which were again found to generate only DBA$^+$ tubules (Figure 5B). Thus, dedifferentiation of NCAM1$^+$ cells *in vitro* may lead in turn to a wider renal potential on grafting *in vivo*.

In Vitro and *in Vivo* Treatment with Anti-NCAM Antibody Drug Conjugate

We next analyzed the effects of depletion of NCAM1$^+$ cells using an anti-NCAM antibody drug conjugate (NCAM-ADC; N901 antibody conjugated to cytotoxic DM1). Initially, we calibrated the cell concentration and ADC concentration required to deplete NCAM1$^+$ cells from proliferative hKEpC cultures (Supplemental Figure S4). As seen from a representative FACS analysis, treatment with NCAM-ADC decreased NCAM1 expression (Figure 6A). Additionally, the MTS proliferation assay showed diminished cell proliferation after ADC treatment, as a result of cell death caused by the immunoconjugate (Figure 6B). Clonogenic capacity and sphere-forming ability of NCAM-ADC–treated cultures were decreased, compared with untreated cells and cells treated with antibody alone (Figure 6, C and D), indicating that depletion of NCAM1$^+$ cells in hKEpCs significantly abrogates stemness traits.

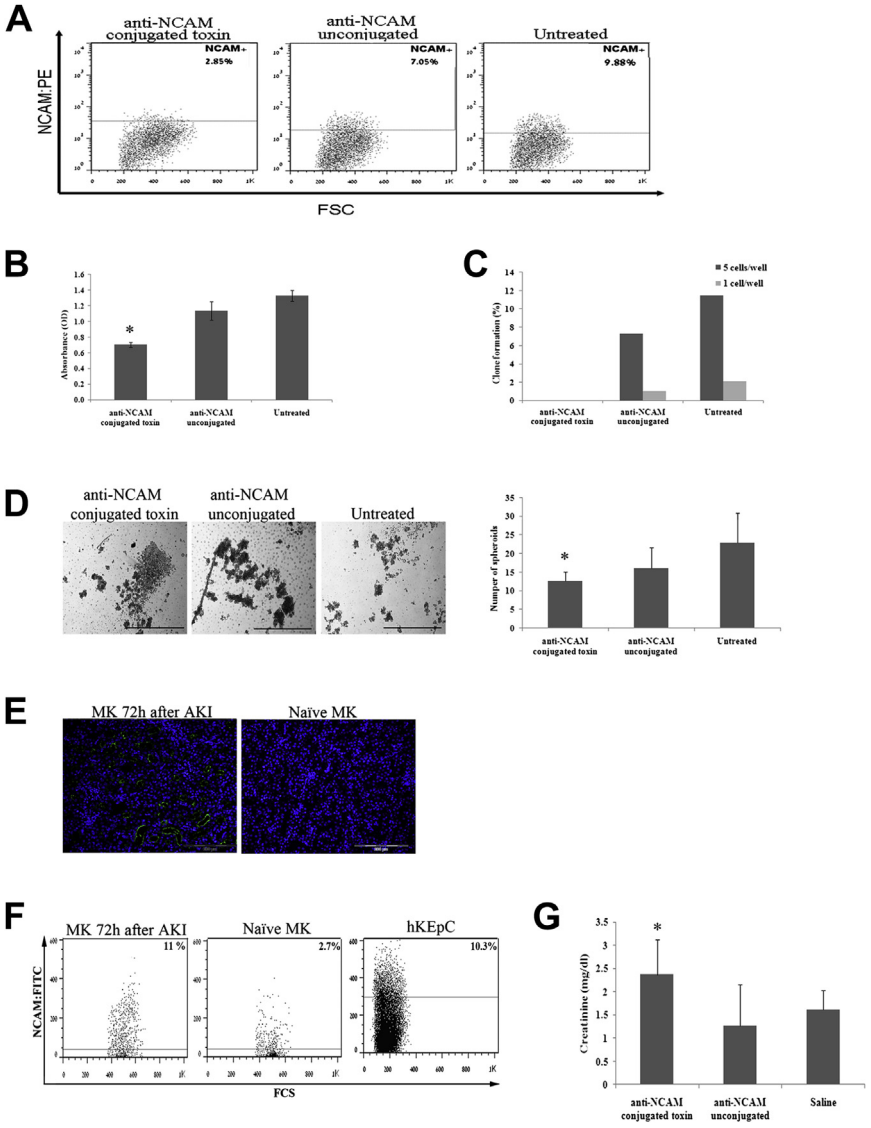

Figure 6 Treatment with anti-NCAM conjugated toxin: hKEpCs treated with anti-NCAM conjugated toxin antibody (huN901-DM1), unconjugated anti-NCAM (huN901) antibody, compared with untreated hKEpCs. **A:** FACS analysis from a representative experiment shows an approximately 30% decrease in NCAM1 expression caused by anti-NCAM conjugated toxin treatment, compared with untreated hKEpCs. Gates were determined according to isotype control in each treatment group separately. **B:** MTS proliferation assay on day 5 of toxin treatment shows a decrease in cell number in the anti-NCAM conjugated toxin antibody treated group. **C:** Clone-formation assay from a representative experiment shows the anti-NCAM conjugated toxin treatment of hKEpCs abolishes clone-formation capacity, in contrast to control and anti-NCAM unconjugated treated groups. **D:** Sphere-formation assay (**left**) shows decreased sphere-formation capacity by hKEpCs treated with the anti-NCAM conjugated toxin, compared with the control and unconjugated anti-NCAM antibody treatment. Sphere numbers were quantified (**right**) for each treatment group. **E:** Mouse kidney staining at 72 hours after glycerol injection shows elevation in NCAM1 endogenous levels, compared with naïve mouse kidney. **F:** FACS analysis of NCAM1 expression shows elevation in NCAM1 levels and binding of the antibody to the mouse cells in injured (AKI) mouse kidney, compared with naïve mouse kidney and hKEpCs using huN901 antibody. **G:** Creatinine blood levels after intravenous administration of the anti-NCAM conjugated toxin to the BALB/c mice 2 hours after glycerol injection. At 72 hours, the creatinine levels are significantly higher, compared with controls. Importantly, unconjugated NCAM N901 antibody, which does not eliminate NCAM1$^+$ cells, counteracts effects of anti-NCAM conjugated toxin, significantly reducing peak renal injury at 72 hours. Data are expressed as means ± SEM of at least three different experiments on three different hKEpCs. *$P < 0.05$. Scale bars: 200 μm (**D** and **E**). MK, mouse kidney; OD, optical density.

Although NCAM1 is not expressed in the resting mature nephron, it reappears in scattered proximal tubular cells after AKI.[28] We therefore evaluated the consequences of eliminating NCAM1$^+$ cells during a regenerative response. We used the glycerol-induced acute tubular injury model in BALB/c mice, in which peak functional renal injury appears 72 hours after glycerol injection and spontaneous recovery occurs thereafter. Similar to our findings for ischemic injury, we found NCAM1 to re-express after toxic tubular injury on the surface of renal epithelia, and up-regulation of NCAM1 levels was readily detected with the NCAM N901 antibody (Figure 6, E and F). NCAM-ADC was administered 2 hours after glycerol injection and renal function was monitored. At 72 hours, renal function was further significantly compromised, compared with controls. Importantly, unconjugated NCAM N901 antibody, which does not deplete NCAM$^+$ cells, counteracted the effects of the NCAM-ADC (Figure 6G).

In Vivo Effects of Human NCAM1$^+$ Cells in Glycerol-Induced AKI

Having established that *in situ* NCAM targeting can modulate renal function during AKI, we tested the effects of exogenous administration of human NCAM1$^+$ cells. We calibrated glycerol-induced AKI in NOD/SCID mice and determined a sublethal injection dose of glycerol (9 μL/g) for further experiments. A control group of mice was used to determine basal levels for serum creatinine and BUN in normal NOD/SCID mice ($n = 12$), which averaged 0.37 ± 0.02 mg/dL and 21.43 ± 2.37 mg/dL, respectively. Similar to injury in BALB/c mice intramuscular injection of glycerol on day 0 resulted in an increase in creatinine and BUN levels, with peak levels observed at 48 to 72 hours. Thereafter, BUN and creatinine levels declined, and spontaneous recovery was observed after 14 days. Intravenously administered NCAM1$^+$ cells (2 hours after glycerol

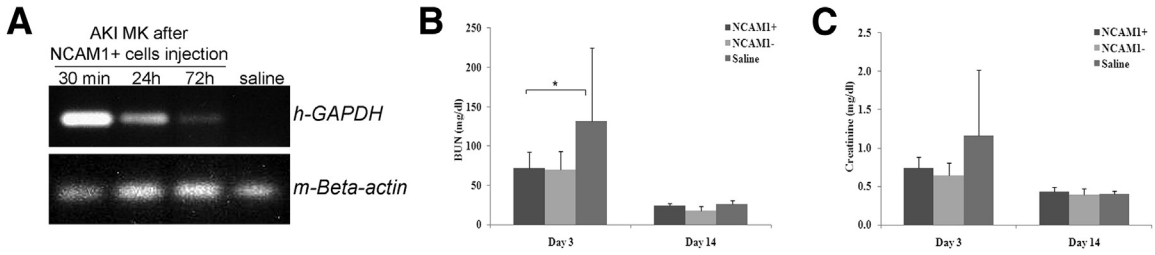

Figure 7 NCAM1$^+$ cells attenuate BUN and creatinine peaks in AKI. NCAM1$^+$, NCAM1$^-$ cells or saline were injected intravenously 2 hours after glycerol administration. **A:** RT-PCR of human specific GAPDH (hGAPDH) of saline-treated mouse kidney (MK) and of mouse kidneys at 30 minutes, 24 hours, and 72 hours after injection of 1×10^6 NCAM1$^+$ cells. Mouse β-actin was used as a positive control for cDNA presence. Blood samples were taken after 3 and 14 days. **B** and **C:** NCAM1$^+$ and NCAM1$^-$ cells attenuate BUN (**B**) and creatinine (**C**) peaks at 3 days, compared with the control (saline) treatment group. The expected spontaneous recovery was observed in all treatment groups at 14 days. Data are expressed as means ± SEM. *$P < 0.05$.

injection) were detected in the kidney at significant amounts within the first 24 hours after injection, but were diminished by day 3 (Figure 7A). NCAM1$^+$ cells did not show exclusive tropism for the injured kidney, but were intensively detectable also in the lungs (Supplemental Figure S5). Analysis of BUN and creatinine levels revealed attenuate BUN peaks (Figure 7B) and tend to attenuate creatinine peaks (Figure 7C) at 3 days, compared with saline-treated mice (Figure 7, B and C). However, there was no significant difference between NCAM1$^+$ and NCAM1$^-$ cells with respect to kidney function in AKI (Figure 7, B and C).

Discussion

Using immunosorting to target the surface marker NCAM1, we identified and characterized a unique population of human kidney stem/progenitor-like cells, which arise from primary cultures of human kidney epithelial cells. This subpopulation could be specifically activated in growing cultures to overexpress embryonic renal stemness markers and could be distinguished in clonal assays, forming large numbers of colonies from single cells in the presence of human FKCM. NCAM1$^+$ cells promptly reverted to a less differentiated mesenchymal-like cell phenotype, down-regulated the expression of mRNAs encoding epithelial markers such as E-cadherin, and up-regulated mesenchymal marker transcripts, but then redifferentiated into epithelial structures in kidney organoids and on grafting as single-cell suspensions into the chick CAM or mouse. Importantly, targeting NCAM1-expressing cells during AKI could modulate disease course.

In embryogenesis, EMT and the reverse process (MET) play central roles.[29–31] Early in development, for example, mesoderm generated by EMTs develops into multiple tissue types; later in development, mesodermal cells give rise to epithelial organs, such as the kidney, a time frame in which NCAM1 is expressed. The loss of E-cadherin expression during EMT is associated with up-regulation of NCAM1 in human breast epithelia, indicating that NCAM1 is a reliable surface marker to identify cells undergoing this process.[32,33] One can therefore take advantage of NCAM1 not only to sort out developmental renal progenitors before completion of epithelialization during the embryonic MET process[13] but also for cells that first emerge during dedifferentiation/EMT in adult human epithelial kidney cells.

When human kidney epithelia are placed in adhesion cultures they are released from normal quiescence to become proliferative hKEpCs. We have repeatedly observed that proliferative hKEpCs, comprising different types of kidney epithelia, are uniformly positive for the CD133/CD24 cell surface markers. CD133/CD24 have been previously suggested as markers of multipotent epithelial stem cells in the kidney.[19,20] Nevertheless, *in vivo* genetic fate mapping has brought into question the presence of such multipotent epithelial stem cells.[34] Moreover, a recent detailed pathological analysis of human kidneys and acute tubular necrosis biopsies suggested, at least for the proximal tubule, that CD133/CD24 are markers of dedifferentiated epithelia rather than a genuine stem cell population.[35] Thus, in terms of *in vitro* precursor relationships, CD133/CD24 mark the entire bulk of proliferating hKEpCs (those that assume some degree of dedifferentiation upon growth in culture), whereas NCAM1 represents the subset that has reverted along the EMT axis to behave in many ways similar to tissue stem cells. Thus, as previously reported for breast epithelial cells,[36] with the present findings we suggest for the first time a link between partial dedifferentiation/EMT and the gain of kidney stem-cell properties leading to a stem/progenitor state *in vitro*.

Our results are interesting in light of previous studies analyzing the cellular events involved in regeneration of renal tubules in animal models. Differentiated tubular cells are thought to dedifferentiate and proliferate after AKI. After enhanced cell proliferation, transiently dedifferentiated regenerating cells are believed to repopulate the damaged area and then redifferentiate into mature epithelial cells to reconstruct the functional integrity of the nephron (reviewed by Bonventre and Yang[37]). This process has been shown to activate developmental programs, including the reappearance of early stem/progenitor cell markers.[9,12,38] Accordingly, NCAM1, which is not expressed in the mature nephron, has been shown to be reactivated in the rat after ischemic injury in the S3 segment of the proximal tubule, an area with a high regenerative response, recapitulating its expression in the developing kidney toward rebuilding the tubule.[28] NCAM1$^+$ cells sorted from proliferative hKEpCs and disclosing a proximal tubular origin may

share similarities with this proximal cell fraction that re-expresses NCAM1 after AKI and is involved in the *in vivo* regenerative response. Interestingly, the tubular structures developed on the chick CAM at 1 week after grafting of human NCAM1$^+$ cells were devoid of renal maturation markers, and differentiation into LTA$^+$ proximal tubules and additional tubule types (not observed with NCAM1$^-$ counterparts) was apparent at 2 weeks in the SCID model. This unique pattern indicates that, when re-establishing the tubule *in situ*, transient reversion of NCAM1$^+$ cells to a presumably early and less committed developmental stage *in vitro* may be followed by stepwise redifferentiation, mimicking renal ontogeny and conferring a wider renal differentiation potential.

Additional parallels can be drawn from experiments with the NCAM antibody drug conjugated, which afforded the opportunity to analyze the consequences of NCAM$^+$ cell depletion, demonstrating both diminished stemness and clonogenic response *in vitro* and worsening of AKI *in vivo*. Thus, NCAM1$^+$ cells activated *in vitro* to acquire stem/progenitor cell characters are likely to be important to the regenerative response that follows AKI *in vivo* and thus represent a target for intervention. The fact that NCAM1 does not express in the resting kidney epithelia further increases its validity as a therapeutic target. Other potential regulators revealed by microarrays to be specific to NCAM-expressing cells include ESRP1 and FGFR2, both of which control developmental pathways and epithelial morphogenesis[22,23] and as such may serve as interventional targets.

Of note, the beneficial effects of exogenous NCAM1$^+$ cells on renal function in the AKI were not exclusive. This lack of exclusive response may be related to the mode of cell administration; with the intravenous route, distribution of cells to the kidney is very limited, and kidney-derived cells arrive and reside in the lungs. This in turn may preclude the differential action of a specific cell subset that is likely dependent on migration to diseased renal tissue and calls for intra-arterial of direct injection modes of cell administration. In addition, it may very well be that any kidney-derived cell exerts some beneficial effect on exogenous delivery. Importantly, the identification of markers of specific cell subsets that participate in the renal regenerative machinery and their *in situ* targeting by peptides, antibodies, and small molecules may be a superior strategy to exogenous cell therapy for AKI.

Supplemental Data

Supplemental material for this article can be found at *http://dx.doi.org/10.1016/j.ajpath.2013.07.034*.

References

1. Weissman I: The ISSCR: who are we and where are we going? Cell Stem Cell 2009, 5:151–153
2. Barker N, van de Wetering M, Clevers H: The intestinal stem cell. Genes Dev 2008, 22:1856–1864
3. Blanpain C, Fuchs E: Epidermal homeostasis: a balancing act of stem cells in the skin. Nat Rev Mol Cell Biol 2009, 10:207–217
4. Kondo M, Wagers AJ, Manz MG, Prohaska SS, Scherer DC, Beilhack GF, Shizuru JA, Weissman IL: Biology of hematopoietic stem cells and progenitors: implications for clinical application. Annu Rev Immunol 2003, 21:759–806
5. Little MH: Regrow or repair: potential regenerative therapies for the kidney. J Am Soc Nephrol 2006, 17:2390–2401
6. Diep CQ, Ma D, Deo RC, Holm TM, Naylor RW, Arora N, Wingert RA, Bollig F, Djordjevic G, Lichman B, Zhu H, Ikenaga T, Ono F, Englert C, Cowan CA, Hukriede NA, Handin RI, Davidson AJ: Identification of adult nephron progenitors capable of kidney regeneration in zebrafish. Nature 2011, 470:95–100
7. Hartman HA, Lai HL, Patterson LT: Cessation of renal morphogenesis in mice. Dev Biol 2007, 310:379–387
8. Pleniceanu O, Harari-Steinberg O, Dekel B: Concise review: kidney stem/progenitor cells: differentiate, sort out, or reprogram? Stem Cells 2010, 28:1649–1660
9. Dekel B, Metsuyanim S, Schmidt-Ott KM, Fridman E, Jacob-Hirsch J, Simon A, Pinthus J, Mor Y, Barasch J, Amariglio N, Reisner Y, Kaminski N, Rechavi G: Multiple imprinted and stemness genes provide a link between normal and tumor progenitor cells of the developing human kidney. Cancer Res 2006, 66:6040–6049
10. Dressler GR: The cellular basis of kidney development. Annu Rev Cell Dev Biol 2006, 22:509–529
11. Rosenblum ND: Developmental biology of the human kidney. Semin Fetal Neonatal Med 2008, 13:125–132
12. Metsuyanim S, Harari-Steinberg O, Buzhor E, Omer D, Pode-Shakked N, Ben-Hur H, Halperin R, Schneider D, Dekel B: Expression of stem cell markers in the human fetal kidney. PloS One 2009, 4: e6709
13. Harari-Steinberg O, Matsuyanim S, Omer D, Gnatek Y, Gershon R, Pri-Chen S, Ozdemir DD, Lerenthal Y, Noiman T, Ben-Hur H, Vaknin Z, Schneider DF, Aronow BJ, Goldstein RS, Hohenstein P: Indentification of human nephron progenitors capable of generation of kidney structures and functional repair of chronic renal disease. EMBO Mol Med 2013, http://doi.dx.org/10.1002/emmm.201201584 [Epub ahead of print]
14. Pode-Shakked N, Metsuyanim S, Rom-Gross E, Mor Y, Fridman E, Goldstein I, Amariglio N, Rechavi G, Keshet G, Dekel B: Developmental tumourigenesis: NCAM as a putative marker for the malignant renal stem/progenitor cell population. J Cell Mol Med 2009, 13: 1792–1808
15. Pode-Shakked N, Shukrun R, Mark-Danieli M, Tsvetkov P, Bahar S, Pri-Chen S, Goldstein RS, Rom-Gross E, Mor Y, Fridman E, Meir K, Simon A, Magister M, Kaminski N, Goldmacher VS, Harari-Steinberg O, Dekel B: The isolation and characterization of renal cancer initiating cells from human Wilms' tumour xenografts unveils new therapeutic targets. EMBO Mol Med 2013, 5:18–37
16. Buzhor E, Harari-Steinberg O, Omer D, Metsuyanim S, Jacob-Hirsch J, Noiman T, Dotan Z, Goldstein RS, Dekel B: Kidney spheroids recapitulate tubular organoids leading to enhanced tubulogenic potency of human kidney-derived cells. Tissue Eng Part A 2011, 17:2305–2319
17. Wang L, Amphlett G, Blättler WA, Lambert JM, Zhang W: Structural characterization of the maytansinoid–monoclonal antibody immunoconjugate, huN901–DM1, by mass spectrometry. Protein Sci 2005, 14:2436–2446
18. Noiman T, Buzhor E, Metsuyanim S, Harari-Steinberg O, Morgenshtern C, Dekel B, Goldstein RS: A rapid in vivo assay system for analyzing the organogenetic capacity of human kidney cells. Organogenesis 2011, 7:140–144
19. Bussolati B, Bruno S, Grange C, Buttiglieri S, Deregibus MC, Cantino D, Camussi G: Isolation of renal progenitor cells from adult human kidney. Am J Pathol 2005, 166:545–555
20. Sagrinati C, Netti GS, Mazzinghi B, Lazzeri E, Liotta F, Frosali F, Ronconi E, Meini C, Gacci M, Squecco R, Carini M, Gesualdo L,

Francini F, Maggi E, Annunziato F, Lasagni L, Serio M, Romagnani S, Romagnani P: Isolation and characterization of multipotent progenitor cells from the Bowman's capsule of adult human kidneys. J Am Soc Nephrol 2006, 17:2443–2456
21. Kuure S, Vuolteenaho R, Vainio S: Kidney morphogenesis: cellular and molecular regulation. Mech Dev 2000, 92:31–45
22. Warzecha CC, Jiang P, Amirikian K, Dittmar KA, Lu H, Shen S, Guo W, Xing Y, Carstens RP: An ESRP-regulated splicing programme is abrogated during the epithelial-mesenchymal transition. EMBO J 2010, 29:3286–3300
23. Warzecha CC, Sato TK, Nabet B, Hogenesch JB, Carstens RP: ESRP1 and ESRP2 are epithelial cell-type-specific regulators of FGFR2 splicing. Mol Cell 2009, 33:591–601
24. Babayeva S, Zilber Y, Torban E: Planar cell polarity pathway regulates actin rearrangement, cell shape, motility, and nephrin distribution in podocytes. Am J Physiol Renal Physiol 2011, 300:F549–F560
25. He F, Xiong W, Yu X, Espinoza-Lewis R, Liu C, Gu S, Nishita M, Suzuki K, Yamada G, Minami Y, Chen Y: Wnt5a regulates directional cell migration and cell proliferation via Ror2-mediated noncanonical pathway in mammalian palate development. Development 2008, 135: 3871–3879
26. Lin S, Baye LM, Westfall TA, Slusarski DC: Wnt5b-Ryk pathway provides directional signals to regulate gastrulation movement. J Cell Biol 2010, 190:263–278
27. Nomachi A, Nishita M, Inaba D, Enomoto M, Hamasaki M, Minami Y: Receptor tyrosine kinase Ror2 mediates Wnt5a-induced polarized cell migration by activating c-Jun N-terminal kinase via actin-binding protein filamin A. J Biol Chem 2008, 283:27973–27981
28. Abbate M, Brown D, Bonventre JV: Expression of NCAM recapitulates tubulogenic development in kidneys recovering from acute ischemia. Am J Physiol Renal Physiol 1999, 277:F454–F463
29. Hay ED: An overview of epithelio-mesenchymal transformation. Acta Anat (Basel) 1995, 154:8–20
30. Pérez-Pomares JM, Muñoz-Chápuli R: Epithelial-mesenchymal transitions: a mesodermal cell strategy for evolutive innovation in metazoans. Anat Rec 2002, 268:343–351
31. Thiery JP, Sleeman JP: Complex networks orchestrate epithelial-mesenchymal transitions. Nat Rev Mol Cell Biol 2006, 7:131–142
32. Lehembre F, Yilmaz M, Wicki A, Schomber T, Strittmatter K, Ziegler D, Kren A, Went P, Derksen PWB, Berns A, Jonkers J, Christofori G: NCAM-induced focal adhesion assembly: a functional switch upon loss of E-cadherin. EMBO J 2008, 27:2603–2615
33. Evseenko D, Zhu Y, Schenke-Layland K, Kuo J, Latour B, Ge S, Scholes J, Dravid G, Li X, MacLellan WR, Crooks GM: Mapping the first stages of mesoderm commitment during differentiation of human embryonic stem cells. Proc Natl Acad Sci USA 2010, 107:13742–13747
34. Humphreys BD, Czerniak S, DiRocco DP, Hasnain W, Cheema R, Bonventre JV: Repair of injured proximal tubule does not involve specialized progenitors. Proc Natl Acad Sci USA 2011, 108: 9226–9231
35. Smeets B, Boor P, Dijkman H, Sharma SV, Jirak P, Mooren F, Berger K, Bornemann J, Gelman IH, Floege J, van der Vlag J, Wetzels JF, Moeller MJ: Proximal tubular cells contain a phenotypically distinct, scattered cell population involved in tubular regeneration. J Pathol 2013, 229:645–659
36. Mani SA, Guo W, Liao MJ, Eaton EN, Ayyanan A, Zhou AY, Brooks M, Reinhard F, Zhang CC, Shipitsin M, Campbell LL, Polyak K, Brisken C, Yang J, Weinberg RA: The epithelial-mesenchymal transition generates cells with properties of stem cells. Cell 2008, 133:704–715
37. Bonventre JV, Yang L: Cellular pathophysiology of ischemic acute kidney injury. J Clin Invest 2011, 121:4210–4221
38. Dekel B, Biton S, Yerushalmi GM, Altstock RT, Mittelman L, Faletto D, Smordinski NI, Tsarfaty I: In situ activation pattern of Met docking site after renal injury and hypertrophy. Nephrol Dial Transplant 2003, 18:1493–1504